Published in final edited form as:
Eur J Neurosci. 2009 January ; 29(1): 132–145. doi:10.1111/j.1460-9568.2008.06567.x.

Engineering angiogenesis following spinal cord injury: A coculture of neural progenitor and endothelial cells in a degradable polymer implant leads to an increase in vessel density and formation of the blood-spinal cord barrier

Millicent Ford Rauch[a], **Sara Royce Hynes**[a], **James Bertram**[a], **Andrew Redmond**[a], **Rebecca Robinson**[a], **Cicely Williams**[a], **Hao Xu**[a], **Joseph A. Madri**[b], and **Erin B. Lavik**[a]

[a]Department of Biomedical Engineering, Yale University 55 Prospect Street, Malone Engineering Center 311, New Haven, CT 06520 USA

[b]Department of Pathology, Yale University 310 Cedar Street, Lauder Hall 115, New Haven, CT 06520, USA

Abstract

Angiogenesis precedes recovery following spinal cord injury (SCI), and its extent correlates with neural regeneration suggesting that angiogenesis may play a role in repair. An important precondition for studying the role of angiogenesis is the ability to induce it in a controlled manner. Previously, we showed that a coculture of endothelial cells (ECs) and neural progenitor cells (NPCs) promoted the formation of stable tubes *in vitro* and stable, functional vascular networks *in vivo* in a subcutaneous model. We sought to test whether a similar coculture would lead to formation of stable functional vessels in the spinal cord following injury. We created microvascular networks in a biodegradable two component implant system and tested the ability of the coculture or controls (lesion control, implant alone, implant plus ECs, or implant plus NPCs) to promote angiogenesis in a rat hemisection model of spinal cord injury. The coculture implant led to a four fold increase in functional vessels compared to the lesion control, implant alone, or implant plus NPCs groups and a 2 fold increase in functional vessels over the implant plus ECs group. Furthermore, half of the vessels in the coculture implant exhibited positive staining for the endothelial barrier antigen, a marker for formation of the blood spinal cord barrier (BSB). No other groups showed positive staining for the BSB in the injury epicenter. This work provides a novel method to induce angiogenesis following SCI and a foundation for studying its role in repair.

Keywords

rat; microvasculature; neural progenitor cells; endothelial cells; hydrogel; scaffold; PLGA; blood-spinal cord barrier

INTRODUCTION

It has been observed that increases in blood vessel density correlate with improvements in recovery in a number of models of spinal cord injury (Glaser et al., 2006; Kaneko et al., 2006; Yoshihara et al., 2007). A similar correlation between the formation of new vessels and recovery has been seen following injury in the central nervous system (CNS) more

*To whom correspondence should be addressed, Tel: 203-432-4263, Fax: 203-432-0030, erin.lavik@yale.edu..

broadly (Hou *et al.*, 2005; Kaneko *et al.*, 2006; Ohab *et al.*, 2006). In systems where regeneration and improvements in functional recovery are seen, greater densities of blood vessels in the spinal cord tissue have been observed independent of the therapeutic paradigm used to promote regeneration (Glaser *et al.*, 2006; Kaneko *et al.*, 2006). Microvessels in the CNS are known to provide tremendous trophic support (Raab & Plate, 2007) as well as be critical for tissue survival (Richardson *et al.*, 2001; Peters *et al.*, 2002). Furthermore, regenerating axons have been shown to grow along blood vessels (Bearden & Segal, 2005). Methods that limit vascular damage, improve vessel density, and restore blood flow to the injured cord may provide a foundation for spinal cord repair and recovery.

New vessels grow rapidly into the lesion site immediately following injury but exhibit significant regression around 14 days post injury (Imperato-Kalmar et al., 1997; Casella et al., 2002; Loy et al., 2002). Some neuroprotective factors have been known to stimulate angiogenesis (Kermani & Hempstead, 2007; Zacchigna *et al.*, 2008) including brain derived neurotrophic factor (BDNF) (Raab & Plate, 2007) which may help to explain the increase in vascular density following its administration after SCI (Patist *et al.*, 2004). Blocking of Sema3A (Kaneko *et al.*, 2006) and administration of bone marrow derived mononuclear cells (Yoshihara *et al.*, 2007) have also been associated with improvements in recovery and greater densities of vessels. While low levels of vascular endothelial growth factor (VEGF), a potent stimulator of angiogenesis, are neuroprotective (Widenfalk *et al.*, 2003) and stimulate angiogenesis following SCI (Facchiano *et al.*, 2002), larger amounts can exacerbate injury by enhancing vessel permeability (Benton & Whittemore, 2003).

Vascular permeability is critical when considering stimulating angiogenesis in the CNS. It is associated with degenerative conditions including multiple sclerosis (Su *et al.*, 2006). Therefore, it is important to stimulate angiogenesis without excessive vascular permeability. The blood brain and blood spinal cord barrier is formed in part by investment of the microvessels with astrocytic end foot processes (Simard *et al.*, 2003) and breakdown of this barrier leads to permeability while formation of the barrier leads to impermeability (Willis *et al.*, 2004). There are a number of methods to assess the formation and breakdown of the blood brain and blood spinal cord barriers including injection of dyes into the vasculature, but one of the more attractive means for assessing the barrier is the use of the endothelial barrier antigen (EBA) (Sternberger & Sternberger, 1987). EBA is present in the majority of microvessels in the healthy spinal cord, but is lost rapidly following injury, and this loss correlates with the permeability of the vessels (Perdiki *et al.*, 1998; Loy *et al.*, 2002). Thus, reformation of the BSB and expression of EBA is a critical component of promoting angiogenesis in the CNS.

In previous work, we found that the implantation of macroporous hydrogels seeded with a coculture of endothelial cells (ECs) and neural progenitor cells (NPCs) led to the formation of functional, stable vessels at long time points in a subcutaneous model (Ford *et al.*, 2006; Rauch *et al.*, accepted). We have found that the NPCs play an important role in forming the stable vessels through a nitric oxide (NO)-mediated pathway (Li *et al.*, 2006), and that the vascular tubes remain stable even after the NPCs are withdrawn (Li *et al.*, 2006). In both *in vivo* models, NPCs were not found at long time points, but the vessels remained stable in contrast to vessels formed from just ECs which showed regression at long time points (Ford *et al.*, 2006; Rauch *et al.*, accepted).

We hypothesized that we could promote angiogenesis following SCI by exploiting the ECs:NPCs coculture system. We constructed a three dimensional microvascular implant seeded with NPCs and ECs in a two component polymer scaffold and tested this system in a hemisection model of SCI. We observed that the coculture of NPCs and ECs in the implant promotes the formation of 3–5 times the number stable functional vessels at the lesion

epicenter as compared to the controls (lesion control, implant alone, implant plus ECs, implant plus NPCs). A second critical step is the formation of a blood spinal cord barrier (BSB). Half of the vessels established a BSB in the coculture seeded implant group. The ECs:NPCs coculture implant increased the density of vessels and promoted the formation of the BSB at the injury epicenter without exacerbating injury. This paradigm leads to an increase in functional vessels with a BSB and provides a new platform for investigating the role of angiogenesis on repair following SCI.

MATERIALS and METHODS

MATERIALS

4-arm poly(ethylene glycol) (PEG, Mn ~ 10,000 g/mol) was from Nektar Therapeutics (Huntsville, AL). Poly(L-lysine) Hydrobromide (PLL, MW 70–150 kDa) was from Sigma (St. Louis, MO). Poly(lactic-co-glycolic acid) (PLGA) Resomer RG 504 (Mn ~ 40,000g/mol) was from Boehringer Ingelheim (Ingelheim, Germany). All media and supplements, 1,1'-dioctadecyl-3,3,3',3'-tetramethylindodicarbocyanine (DiI), and secondary antibodies were from Invitrogen Technologies (Carlsbad, CA). Epidermal growth factor (EGF) was from BD Biosciences (Bedford, MA) and 10% neutral buffered formalin was from Polysciences, Inc. (Warrington, PA). Nylon mesh was from Sefar (Monterey Park, CA).

METHODS

Implant Fabrication and Characterization—The implant is a two component system which incorporates a PLGA 504 oriented outer scaffold and a macroporous PEG/PLL hydrogel inner scaffold. The PLGA oriented scaffold was fabricated as described in Teng et al. (Teng *et al.*, 2002). The macroporous hydrogel was fabricated using PEG and PLL macromers as previously described (Hermanson, 1996; Ford *et al.*, 2006; Rauch *et al.*, accepted). We evaluated the morphology of the scaffolds using scanning electron microscopy (SEM, FEI XL-30 environmental, 5kV).

Cell Maintenance and Seeding—Green fluorescent protein (GFP) neural progenitor cells (NPCs) were isolated from the subventricular zone (SVZ) of postnatal day 1 (P1) transgenic GFP rats, SD-Tg(CAG-EGFP)CZ-004Osb, and maintained following (Morshead *et al.*, 1994; Lu *et al.*, 2002). NPC neurospheres were maintained in DMEM/F12 media containing 20 ng/ml EGF, 1 mM L-glutamine, 1% N2 supplement, 1% B27, and 1% penicillin/streptomycin with fungizone and passaged (1:2) every 2 weeks. The transgenic GFP rats were a kind gift of Dr. Masaru Okabe (Osaka University, Japan) and Dr. Jeffrey Kocsis (Yale University, New Haven, CT). All animal procedures followed the NIH guidelines for animal care and safety and were approved by the Animal Care and Use Committee of Yale University.

Endothelial cells (ECs) were isolated from the epididymal fat pads (Madri & Williams, 1983) of Sprague Dawley rats and cultured in DMEM containing 10% FBS, 5% bovine aortic endothelial cell conditioned medium, 10 mM HEPES, 1mM sodium pyruvate, 1mM L-glutamine, and 1% penicillin/streptomycin.

Hydrogels were cut to 1 mm × 3 mm × 4 mm and seeded with a coculture of NPCs:ECs at a ratio of 1:10 (1 million ECs and 100,000 NPCs per implant at a concentration of 1.1×10^6 cells/ml) (n = 14) for 1 day, low passage ECs (1 million cells per gel at a concentration of 1×10^6 cells/ml) (n = 11) for 1 day, or low passage NPCs (100,000 cells at a concentration of 1×10^5 cells/ml) (n = 12) for 7 days. 7 days was found to give the optimal attachment and density of NPCs in the gels. NPC media was changed at days 4 and 7. The NPC:EC group and EC group were cultured in EC media at 37°C and 5% CO_2 for 1 day. Longer times in

culture resulted in a reduction in the number of EC tubes most likely due to the production of MMPs by rat ECs (personal communication, JA Madri). PLGA oriented scaffolds were cut to dimensions of 0.5 mm × 3 mm × 4mm and were sterilized by soaking in 70% ethanol overnight followed by three washes with PBS prior to implantation.

***In vitro* Quantification of NPC Number and Differentiation—**The *in vitro* seeding methods and culture conditions replicate those for the preparation of the implants for the spinal cord study. The implant plus NPCs group (n = 4), implant plus ECs group (n=3), and NPCs:ECs coculture group (n = 4) were seeded.

To determine the total number of cells on the gels, the NPC group, EC group, and the NPCs:ECs group were evaluated using the Cell Titer-Blue Viability Assay (Promega, Madison, WI) at 1 day or 7 days using Promega's standard protocol. The number of NPCs in the NPC:EC coculture was determined by subtracting the scaffold plus EC values from the scaffold plus NPCs:ECs values.

Cell-seeded gels were fixed in 10% formalin for one hour and soaked in 30% sucrose overnight. **Gels were cryosectioned into 20** μm cross sections and were immunostained for nestin (mouse monoclonal anti-nestin from ascites fluid purified by affinity chromatography, BD Pharmingen, catalogue # 611658, 1:200), glial fibrillary acidic protein (GFAP, rabbit anti-GFAP, Sigma, catalogue # G9269, 1:160), ®$_{III}$ **tubulin (**®$_{III}$ **tub, mouse monoclonal anti-**®$_{III}$ tubulin, Promega, catalogue # G7121, 1:1000), and neurofilament 200 (NF, rabbit anti-Neurofilament 200, Sigma, catalogue #N4142, 1:80). Secondary antibodies were goat anti-rabbit Alexa Fluor 647 (Molecular Probes, catalogue #A-21244, 1:200), and goat anti-mouse Alexa Fluor 647 (Molecular Probes, catalogue #A-21235, 1:200). Samples were blocked in 5% BSA and 3% normal goat serum (Vector Laboratories) for one hour at room temperature followed by incubation with the primary antibody overnight at 4°C and then incubation with the appropriate secondary antibody for one hour at room temperature. Normal spinal cord tissue was used as the positive control for the antibodies and muscle sections were used as negative controls.

Three samples from the NPCs and NPCs:ECs groups were sectioned, and 10 representative images from 3–5 sections were acquired for each antibody using the using a 20X objective (Zeiss, N.A. = 0.75) on a Zeiss Axiovert 200 Inverted Microscope with a MRm camera and Axiovision 4.4 software. Differentiation was quantified by dividing the area positive for each antibody by the total cell area of GFP-positive NPCs following (Hynes *et al.*, 2007).

Surgical Procedures and Animal Care—Fifty nine female Sprague Dawley rats (Charles River Laboratories, Wilmington, MA) weighing approximately 180–200 grams were used. Rats were anesthetized with an intraperitoneal injection of ketamine (60 mg/kg) and xylazine (10 mg/kg). Using aseptic technique, an incision was made over the mid-thoracic vertebrae followed by a laminectomy at the 8th–9th thoracic vertebrae and a 4 mm lateral hemisection at the T9-T10 level. The dorsal artery was cauterized to prevent extensive bleeding. The surgeon then used a no. 11 surgical blade to make a 4 mm long cut along the mid-line of the spinal cord and used microscissors to cut the rostral and caudal ends of the left side of the cord. The tissue was removed with fine forceps and gelfoam was inserted into the cavity to facilitate hemostasis. After the hemisection, the surgeon and an independent observer visually confirmed no residual nerve fibers remained in the cavity. The observer further confirmed the position and size of the lesion with a ruler and then provided the surgeon with the treatment. The surgeon was blinded to the treatment up to this point. Except in the lesion control, the macroporous gel was first inserted into the cavity adjacent to the unlesioned tissue. The PLGA scaffold was then inserted tightly against the gel and the facets on the outer edge of the spinal column.

Five treatment groups were examined in this study: lesion control (n = 11), implant alone (n = 11), implant plus NPCs (n = 12), implant plus ECs (n = 11), and implant plus NPCs:ECs (n = 14). On each surgical day, all of the treatments were performed to minimize differences between groups, control for any changes in surgical technique during the study, and allow the surgeon to remain blinded to the treatments prior to their administration. All animals received 10 ml of lactated Ringer's solution, 5 mg/kg gentamicin, and 10% cranberry juice for 1 week post-injury. Animal bladders were expressed twice daily until bladder function was recovered (7–14 days) (Benton & Whittemore, 2003).

All animal procedures followed the NIH guidelines for animal care and safety and were approved by the Animal Care and Use Committee of Yale University.

Tissue Processing for Histology and Immunocytochemistry—Two animals (1 implant plus ECs group and 1 implant plus NPCs:ECs group) were sacrificed at three weeks post injury to observe vessel formation. The remaining fifty-seven animals were sacrificed at 56 days post injury (DPI).

Following an overdose of ketamine and xylazine, animals received tail injections of 250 μl of 2 mg/ml biotinylated tomato (Lycopersicon esculentum) lectin (Vector Labs, Burlingame, CA) in PBS. Ten minutes later, animals were transcardially perfused with 4% paraformaldehyde (PFA).

Spinal cords were dissected and post-fixed overnight in 4% PFA at 4°C. Tissue was rinsed with 1X PBS and soaked in 30% sucrose overnight at 4°C. Tissue was frozen in a 1:1 mixture of isopentane and liquid nitrogen. One centimeter blocks which included the injury epicenter were embedded in OCT and cryosectioned to 20 μm cross sections (n = 5 for each group) and 20 μm longitudinal sections (n = 4 for each group).

Representative spinal cord tissue was stained and quantified from each group. Spinal cords were chosen from animals whose behavior scores placed them near the mean of their respective group. Twenty micron cross sections were stained with streptavidin-Texas Red-X (Invitrogen, catalogue #S-6370, 1:200), and antibodies to: rat endothelial cell antigen-1 (RECA-1, mouse anti-RECA-1, Abcam, catalogue #ab9774, 1:100), platelet endothelial cell adhesion molecule-1 (PECAM-1, rabbit anti-PECAM-1, a generous gift of Dr. Peter Newman, Blood Center of Wisconsin (Mahooti *et al.*, 2000), 1:400), laminin-1 (rabbit anti-laminin, Sigma, catalogue #L9393, 1:60), endothelial barrier antigen (EBA, mouse anti-EBA, Covance Innovative Antibodies, catalogue #SMI-71R, 1:1000), GAP-43 (mouse anti-GAP-43, Sigma, catalogue #G9264, 1:2000), and neurofilament 200 (NF, Sigma, 1:80). Secondary antibodies were goat anti-rabbit Alexa Fluor 647 (Molecular Probes, catalogue #A-21244, 1:200), and goat anti-mouse Alexa Fluor 647 (Molecular Probes, catalogue #A-21235, 1:200). Normal spinal cord tissue was used as the positive control for the antibodies and muscle sections were used as negative controls. Sections were also stained with hematoxylin and eosin (H&E) and eriochrome cyanine (ECy) (Kiernan, 1984).

Quantification of myelin sparing—Eriochrome cyanine staining (ECy) was used to visualize myelin preservation (white matter spared) in spinal cord tissue cross-sections. Five cords were analyzed per treatment group. Images were taken with a Q imaging Qicam using a MONO 10-bit lens (4X objective, N.A.= 0.1) on an Olympus IX71 Fluorescent Microscope with QCapture Pro (Version 5.1.1.14) and analyzed with Axiovision 4.4 software. The 4X objective permitted the entire spinal cord cross-section to be observed in the field of view.

White matter spared was determined using Axiovision to measure the area stained with ECy. The area of spared white matter was measured at the epicenter and throughout the degenerated tissue following (Widenfalk *et al.*, 2001; Iannotti *et al.*, 2004). The lesion epicenter was the section with the least amount of spared white matter. The area of white matter spared foreach section at 600 micron intervals from the epicenter was quantified. Summary data are presented as means ± S.E.M.

Quantification of Blood Vessels—A 5X objective (Zeiss, N.A. = 0.25) was used to observe the entire cross section on a Zeiss Axiovert 200 Inverted Microscope with an MRm camera and Axiovision 4.4 software. For each section, an ellipse based on the circumference of the remaining tissue on the uninjured side was made and bisected to delineate the injured and uninjured sides. Images were then acquired using a 20X objective (Zeiss, N.A. = 0.75) on either the injured or uninjured sides based on the bisection of the ellipse. Except in the case of the lesion control, we were also able to confirm whether we were acquiring images on the injured side by insuring that we were to the injured side of the interface between the remnants of the hydrogel and the spinal cord tissue. Three images were acquired at each location from three cords from each group (Skold *et al.*, 2000; Facchiano *et al.*, 2002).

Functional blood vessels were identified by their positive staining with streptavidin-Texas Red, which binds to the biotinylated tomato lectin in perfused vessels. In this work, we define functional vessels as those that have successfully anastamosed to host vessels. This is an important first step in forming a functional vasculature following SCI. The vessel diameter was measured from outer cell body to opposite outer cell body normal to the length of the tube using established techniques (Ogunshola *et al.*, 2000; Loy *et al.*, 2002; Ford *et al.*, 2006). The density of vessels was calculated by determining the number of vessels per viewing area of a 20X field (430 μm by 340 μm) using established methods and definitions (Richardson *et al.*, 2001; Loy *et al.*, 2002). To quantify vessel density beyond the lesion epicenter, images further rostral and caudal were taken in the grey matter on the lesioned and unlesioned side. In addition to using biotinylated lectin staining to quantify vessel density, vessel density was confirmed with PECAM-1 staining (n = 5 for each group).

Images of EBA-positive vessels were acquired and quantified using an identical procedure to that outlined above (n = 5 for each group). Data are presented as means ± S.E.M.

Quantification of NPC number and differentiation in vivo—To quantify the number of surviving GFP-positive NPCs, the area of FITC-positive cells was measured in each section in which NPCs were observed. This total cell area was then divided by the average cross-sectional area of one NPC to approximate the total number of surviving NPCs. Because the distance between each sister section was 20 μm and we only measured the FITC-positive area that co-localized with cell nuclei, we avoided counting cells more than once.

This method was also used to quantify the number of nestin, GFAP, β_{III} tubulin, and NF-positive NPCs. Knowing the total number of NPCs observed in each cord, we were able to determine the percentage of cells positive for each antibody. Confocal images were acquired with a Zeiss Axiovert 100/ LSM 510 Meta confocal laser scanning microscope and LSM 510 software. We used a 40X water immersion objective (N.A. = 1.2) with a laser to excite the GFP fluorophore (excitation at 488 nm) and the Alexa Fluor 647 fluorophore (excitation at 633 nm). Sections were scanned at 1 μm intervals and using LSM 510 software images were averaged to optimize fluorescent signals and decrease noise. Confocal microscopy confirmed whether GFP and the antibodies co-localized.

Quantification of NF at the implant interface—NF at the implant interface was quantified using longitudinal sections by acquiring three images at midline and at the rostral and caudal ends of that scaffold for each cord.

Statistics—Data were analyzed using a one-way or two-way analysis of variance (ANOVA) followed by the Neuman-Keuls multiple comparisons post test when the ANOVA showed that significant differences were present. Differences were accepted as statistically significant with $p < 0.05$. Summary data are presented as means ± S.E.M.

RESULTS

Implant design and architecture

We fabricated a two component implant for the hemisection study based on a PLGA outer scaffold which has been shown to reduce glial scarring (Teng *et al.*, 2002) and a macroporous inner hydrogel scaffold which supports the coculture of NPCs and ECs leading to the formation of stable vessels (Ford *et al.*, 2006; Rauch *et al.*, accepted) (Fig. 1a). After seeding the macroporous hydrogel with ECs or a coculture of NPCs and ECs, ECs form multicellular aggregates, or tubes, along the macropores of the gel (Fig. 1b, d). By quantifying the density of tubes in the implants just prior to implantation, we determined that 18 ± 2 tubes/mm^2 are implanted in the EC group and 13 ± 1 tubes/mm^2 are implanted in the NPC:EC group (Fig. 1e). The density of tubes at the time of implantation appears to be a function of the density of pores in the macroporous gel (Rauch *et al.*, accepted).

White matter sparing and General Pathology

Figure 2 (a–f) shows the white matter spared rostral, at, and caudal to the injury epicenter in representative sections for the lesion control and implant plus NPCs groups. There were no differences in the amount of white matter spared rostral to, at, or caudal to the epicenter between the groups, and the lesion area as measured using the ECy was the same for all of the groups. At the epicenter, there is a ring of white matter, and in some cases, some potential grey matter, albeit very little. The grey matter is more evident in the hematoxylin and eosin (H&E) staining (Fig 2k and Fig 2l).

The tissue in all groups shows significant signs of degeneration even 3 mm rostral and caudal to the epicenter. In both the lesion control and implant plus NPCs tissue in Fig. 2 one can see signs of cysts and scar tissue 3 mm rostral and caudal to the epicenter on the lesioned side of the cords.

The H&E results mirror those seen with ECy. The lesioned side of the cords (to the left in Fig. 2j–l and on the top in Fig. 2m–n) shows signs of degeneration. The unlesioned side is more intact but there is little grey matter present at the injury epicenter. The scaffold can also be visualized in H&E. In figure 2n, one can see the remains of the hydrogel component of the implant. The PLGA outer scaffold has degraded completely. The hydrogel, which degrades by enzymatic hydrolysis, remains present in part at this time point.

Increases in the density of functional vessels with the coculture at the lesion epicenter

By injecting biotinylated tomato lectin through the tail vein just prior to perfusion, we labeled only vessels that anastomosed with the host vessels (Lee *et al.*, 2002). In this work, we have defined vessels as functional to be those that are anastomosed to differentiate them from vessels that are present but have not inosculated with the host. Anastamosis is one of the crucial steps in achieving vessel functionality in an implant. Regardless of group or location, all of the tomato lectin-labeled vessels were of similar size, approximately 6 μm in

diameter. Fig. 3 (a–d) shows representative images of the vessels across the groups with low magnification images to orient the viewer.

While there were functional vessels present in the lesion epicenter for all of the groups there were significantly more vessels in the implant plus NPCs:ECs group compared to the lesion control ($p<0.01$) and implant alone ($p<0.001$) groups (Fig. 3e) (ANOVA, F statistic 9.745, degrees of freedom, 4 between groups and 41 within groups). In fact, there were 3.5 times more vessels than the implant alone and 5 times as many vessels in the lesion control groups. Analysis of vessels on the unlesioned side of the injury epicenter demonstrated a trend towards increased vessel densities with the implant or implant plus cells; however, there were no statistical differences between the groups (Fig. 3f).

The vessels in the lesion epicenter were also positive for RECA-1 (Casella *et al.*, 2002; Loy *et al.*, 2002), and PECAM-1, an endothelial marker that organizes at cell-cell junctions (Pinter *et al.*, 1999) (Fig. 3g). We also determined the density of vessels by quantifying PECAM-1 positive vessels and the values were similar suggesting that the vast majority of the vessels are inosculated with the host.

Vessel density was also measured rostral and caudal to the lesion epicenter in the grey matter. Vessel densities increased moving rostral and caudal from the lesion epicenter and approached the vessel density for normal grey matter, approximately 400 vessels/mm^2 (Blight, 1991), at 3.6 mm rostral and 3.6 mm caudal to the lesion epicenter for all of the groups (Fig. 3h and 3i).

Two animals (n = 1 from the implant plus ECs group and n = 1 from the implant plus NPCs:ECs group) were sacrificed at three weeks post injury to investigate changes in vessel density at an intermediate time point. Vessel regression has been seen in a number of models of angiogenesis (Benjamin, 2000; Gosain *et al.*, 2006) as well as after SCI (Loy *et al.*, 2002). Biotinylated tomato lectin was not injected in animals sacrificed at 3 weeks, so immunostaining for PECAM-1 and laminin-1 was used to characterize the blood vessels present at 3 weeks (Fig. 4). The implant plus NPCs:ECs animal had 57 ± 12 vessels/mm^2 PECAM-1 positive vessels at 3 weeks. In comparison, at 8 weeks, the implant plus NPCs:ECs group had 50 ± 8 vessels/mm^2. Likewise, at 3 weeks, the implant plus ECs animal had 59 ± 9 PECAM-1 vessels/mm^2 at the injury epicenter. At 8 weeks, the implant plus ECs group had 32 ± 8 vessels/mm^2. The values at 3 weeks are within the standard deviation of the 8 week data for both groups suggesting, albeit with a small sample size, that the vessel density is the same between 3 weeks to 8 weeks. The presence of laminin around the vessels is consistent with mature vessel matrix which further supports the thesis that the vessels are stable.

Vessels positive for endothelial barrier antigen in the coculture group

To evaluate whether vessels at the injury epicenter established a BSB, we stained spinal cord tissue for EBA (Sternberger & Sternberger, 1987; Loy *et al.*, 2002). All of the groups demonstrated some EBA-positive vessels on the unlesioned side at the lesion epicenter (Fig. 5a, c, d). However, only the implant plus NPCs:ECs group had EBA-positive vessels on the lesioned side at the injury epicenter (Fig. 5b, c, d). The number of EBA-positive vessels on the lesioned side for the implant plus NPCs:ECs group was 18 ± 6 vessels/mm^2. No vessels were found on the injured side at the injury epicenter for any of the other groups.

This suggests that the NPCs:ECs coculture plays a role in promoting the formation of the BSB. However, while approximately 70% of the NPCs were found to be GFAP positive and appeared to be investing vessels, we did not find colocalization of NPCs with the EBA immunostaining.

The behavior of the NPCs: their survival and differentiation

GFP expressing NPCs were still present in the spinal cord at 8 weeks post implantation (Fig. 6). NPCs were found in 2 of the 14 cords in the implant plus NPCs:ECs group and in 3 of the 12 cords in the scaffold plus NPCs group. No NPCs were observed in the NPCs:ECs animal sacrificed at 3 weeks. The majority of NPCs were observed in clusters in or near the implant at the lesion epicenter and in close proximity to blood vessels (Fig. 6b). Longitudinal sections showed that NPCs migrated up to 100–200 μm from the lesion epicenter both rostrally and caudally into tissue ipsilateral and contralateral to the initial hemisection.

Approximately 14,000 NPCs were transplanted in the implants plus NPCs group and approximately 3000 NPCs (~20 % of NPCs transplanted) were found at 8 weeks (Fig. 6a). Approximately 9800 NPCs were transplanted in the implant plus NPCs:ECs group and approximately 800 NPCs (~8 % of NPCs transplanted) were found in the implant plus NPCs:ECs group at 8 weeks (Fig. 6a).

The majority of GFP positive NPCs that survived were nestin and GFAP positive (Fig. 6c–k). The nestin positive cells exhibited immature morphologies lacking processes. Some of the GFAP positive NPCs appeared to be investing what could be blood vessels (Fig. 6f). A large number of the NPCs exhibited coexpression of nestin and GFAP staining similar to that observed *in vitro* (Fig. 2q and 2r) which is commonly seen in immature NPCs (Gates *et al.*, 1995; Engelhardt *et al.*, 2004). Images also showed limited NPC differentiation to β_{III} tubulin positive neurons in the implant plus NPCs group (1.2% ± 0.7) and the implant plus NPCs:ECs group (0.15% ± 0.1) (Fig. 6i–k, l). β_{III} tubulin positive NPCs were found in the implant at the injury epicenter among nestin and GFAP positive cells. No NPCs were found to be NF-positive.

Vessels lead to greater NF and upregulation of GAP-43

NF positive fibers were present in all of the groups at the injury epicenter with the majority of NF staining being on the unlesioned side of the cords. NF positive cells exhibited long, thin, branching processes. Quantification of NF immunostaining showed an increase in the area of NF staining in the presence of the implant for the implant plus NPCs ($p<0.05$) and implant plus NPCs:ECs groups ($p<0.001$) compared to the lesion control group (Fig. 7a–c) (ANOVA, F statistic 8.303, degrees of freedom, 4 between groups and 37 within groups). The implant plus ECs did not lead to a statistically significant increase in NF staining overall, but as described below, it appeared to affect NF sprouting into the implant.

NF fibers were also quantified at the spinal cord/implant interface. The interface could be identified due to the presence of the hydrogel at 8 weeks post implantation (Fig. 7g). Cords from the lesion control group were not included in the quantification; however there was no NF positive tissue at the lesion/spinal cord interface. Fibers were seen growing into the implants from the rostral, caudal and contralateral spinal cord tissue in all of the implant groups. Quantification of the ingrowth of NF fibers from the rostral and caudal portions of the interface show a trend for increased ingrowth in the implant plus ECs and implant plus NPCs:ECs groups compared to the implant alone. Quantification of the total implant interface showed significantly greater NF immunostaining for the implant plus ECs and implant plus NPCs:ECs groups compared to the implant alone groups Fig. 7d) (ANOVA, F value 3.722, degrees of freedom, 3 between groups and 61 within groups). These groups also had significantly greater densities of vessels at the injury epicenter (Fig. 3e).

Fig. 7g is a representative longitudinal section from the implant plus NPCs group and it is a sister section to the cord in Fig. 2n. There are NF fibers throughout the cord as well as GFP-positive NPCs are present in the implant. Rostral and caudal to the injury epicenter, NF

positive neurons exhibited a classic linear morphology in the uninjured white matter, while at the injury epicenter NF fibers were more tortuous in appearance. NF fibers on the lesioned side at the injury epicenter are not from differentiated NPCs, but appear to sprout from the host. GAP-43, a protein upregulated in the growth cone of regenerating axons (Benowitz et al., 1988), was used to elucidate whether NF fibers were spared or sprouting. We observed GAP-43-positive axons at the injury epicenter as well as further from the epicenter in the white and grey matter for all treatment groups. GAP-43 cells had long, thin fibers. In the implant groups, GAP-43 fibers appeared to sprout from the contralateral side into the implant (Fig. 7f) as well as from the rostral and caudal tissue into the lesion epicenter. Similar to NF, GAP-43 fibers had a tortuous morphology at the injury epicenter. No NPCs showed colocalization for GAP-43. For the two animals (1 implant plus ECs and 1 implant plus NPCs:ECs) that were sacrificed at 3 weeks, there were no differences in NF or GAP-43 staining compared to their respective groups at 8 weeks. NF and GAP-43 fibers were observed in the lesion and appeared to sprout from the host into the injury epicenter.

DISCUSSION

The polymer implant reduced glial scarring (please see supplementary information) and the inflammatory response (please see supplementary information) as compared to the lesion control. It has the capacity to modify the injury environment which is critical in promoting repair. In this case, it provided an environment that is permissible to inosculation of vessels and angiogenesis following SCI. The coculture of NPCs and ECs in the polymer implant led to a 3–5 fold increase in the number of functional vessels at the lesion epicenter at 8 weeks compared to the control groups. In designing the study, cell only controls were not included. Tissue engineered constructs improve cell survival (Langer & Vacanti, 1993; Tomita et al., 2005). Moreover, scaffolds provide architectural control to direct cells to form tissue like structure that differ substantially from cell alone treatments (Langer & Vacanti, 1993; Lavik & Langer, 2004). We have previously shown that a three dimensional gel is important in promoting EC vessel formation in vivo (Ford et al., 2006; Rauch et al., accepted). We implanted approximately 15 tubes/mm^2 in the implant plus ECs and implant plus NPCs:ECs groups. At 8 weeks post implantation, there were approximately 30 vessels per mm^2 in the implant plus EC group and 50 vessels per mm^2 in the implant plus NPCs:ECs group. In the implant plus NPCs group and implant alone groups, there were no tubes at the time of implantation and the implant alone and implant plus NPCs groups had only 5–10 vessels per mm^2. While angiogenesis into the implants occurred to a degree in all of the groups, the implantation of the coculture led to a significant increase in the density of vessels. Furthermore, this increase in vascular density occurs as early as 3 weeks post injury suggesting that the coculture promotes vessel formation early in the recovery process.

There are several possible mechanisms by which the coculture could increase vessel density. A coculture of NPCs and ECs is thought to promote vessel stabilization by the active modulation of angiogenic factors. In both an *in vitro* culture model and *in vivo* subcutaneous model, we observe increases in vessel density when there is a coculture of NPCs and ECs (Ford et al., 2006; Li et al., 2006; Rauch et al., accepted). In the *in vitro* coculture of NPCs and ECs, NPCs secrete NO which induces EC production of VEGF and BDNF which in turn stimulate NPCs to produce more NO (Li et al., 2006). This promotes EC vessel formation and stabilization (Ford et al., 2006; Li et al., 2006). In the subcutaneous mouse and rat models, the coculture of ECs and NPCs leads to a greater density of vessels at long time points compared to ECs or NPCs alone in the gel (Ford et al., 2006; Rauch et al., accepted). When ECs were seeded alone in the gel *in vivo*, vessel regression was seen after 4 weeks. Such regression was not seen in the coculture even though the NPCs could not be found at the long time points. The system not only provides tubes as a basis to build vessels but it

may also provide the biological cues to stimulate angiogenesis and, ultimately, lead to the formation of greater densities of vessels.

All of this is occurring after a significant injury. While the intricate organization of the spinal cord is not recapitulated, it is promising that we are able to begin to build significant numbers of vessels, even in this highly compromised injury environment. Furthermore, this increase in vascularity occurred without exacerbating the injury. The lesion size was comparable for all of the groups and behavioral testing and performance were likewise identical (please see supplementary materials). Thus, this technique provides a new platform to look at the role of angiogenesis and microvessels following SCI.

One question that remains is what contribution the host vasculature makes to vessel formation, namely which endothelial cells are donor versus host cells. In our experiments we did see host vessels infiltrating in the NPC alone group suggesting that the host vessels play an important role in the overall density. It is likely in the EC containing groups that the majority of new vessels are chimeric in nature with both host and donor ECs in the vessels as has been seen previously following implantation of vascular structures (Nor *et al.*, 2001; Tremblay *et al.*, 2005; Mondrinos *et al.*, 2008). The implantation of the donor cells can play a role in creating the appropriate chemical environment to direct the host response (Caplan & Dennis, 2006).

Approximately 10–20 percent of the NPCs survive following transplantation in the NPCs:ECs and NPCs alone groups. In our previous work, we found that the NPCs needed to be present only transiently in the coculture to stimulate the stabilization of the vessels (Ford *et al.*, 2006; Li *et al.*, 2006; Rauch *et al.*, accepted), and here we see similar vessel densities regardless of whether we find NPCs at the 8 week time point. This further suggests that the NPCs are needed only transiently to stimulate angiogenesis. The majority of the surviving NPCs were found around blood vessels. In fact, there appears to be a close association of the NPCs with the vasculature and in some cases, the NPCs may be investing blood vessels.

It is interesting that a greater percentage of the NPCs survive in the NPC plus implant group than in the coculture group even though the coculture group has significantly more blood vessels present. A greater number of NPCs were implanted in the NPC plus implant group. NPCs are known to produce a number of survival factors (Lu et al., 2003), and it may be that there is a critical density of NPCs that leads to a more favorable environment for survival. Increases in seeding density have been associated with greater survival of transplanted neural cells in other models (Terpstra et al., 2007), and we may be seeing a similar effect here.

The majority of NPCs remain both nestin and GFAP-positive as has been seen in other studies (Cao *et al.*, 2001; Teng *et al.*, 2002; Pallini *et al.*, 2005) (Fig. 6). However, some NPCs (1.2% of the total NPCs observed in the cord in the implant plus NPCs group) stain positively for β_{III} tubulin, a marker for relatively immature neurons. The PEG/PLL gel, the inner scaffold in this work, promotes neuronal differentiation of NPCs *in vitro* (Hynes *et al.*, accepted). Since less NPC neural differentiation occurs in the spinal cord as compared to NPC differentiation in the macroporous gel *in vitro*, it is possible that the cues within the SCI environment restrict neural differentiation (Cao *et al.*, 2001). While NPCs could down-regulate GFP upon differentiation, it is unlikely. Differentiated cells from an identical GFP rat strain express GFP up to 8 weeks (Sasaki *et al.*, 2006).

For blood vessels to be functional following SCI, they must not only be perfused but must also form a stable BSB to restrict the movement of large molecules into the CNS and allow for normal neural function (Mautes *et al.*, 2000). Disruption of the BSB leads to vascular permeability and contributes to the secondary injury processes of SCI (Mautes *et al.*, 2000;

Whetstone *et al*., 2003). We found that the coculture was the only treatment that led to the expression of the marker for the BSB on the lesioned side of the cord. Approximately half of the vessels in the coculture group were EBA-positive, one of the major markers for the BSB (Ghabriel *et al.*, 2002; Loy *et al.*, 2002). In contrast, none of the other groups have any EBA-positive vessels on the lesioned side at 8 weeks post injury. This finding suggests that the coculture may play a role in the reformation of the BSB. GFAP-positive NPCs appear to be investing vessels (Fig 6 f–h), and this could play a role in the reformation of the BSB, although we found no direct evidence showing colocalization of NPCs with EBA-positive staining. It is also possible that the NPCs provide trophic support that promotes investment by host astrocytes. While the mechanism clearly should be investigated, it is exciting to see the expression of one of the markers for the BSB. There is limited evidence from other studies that the BSB can be reestablished post SCI (Loy *et al.*, 2002), suggesting that the coculture may be a new means to investigate not only vessels but the reformation of the BSB following SCI.

Ultimately, our goal is to use this new technique to stimulate the formation of new vessels to study their role in repair following SCI. While we do not see massive regeneration, we do see a greater degree of sprouting into the epicenter that correlates with greater densities of vessels. This encouraging finding supports the thesis that angiogenesis may play an important role in creating an environment that promotes repair.

CONCLUSION

Angiogenesis may play an important role following SCI, and we have developed a new system to look at the role of microvessels and the BSB following injury. Our two component polymer implant plus NPCs:ECs promoted the formation of stable, functional vessels with a large number of those vessels exhibiting a positive marker for the BSB. This work demonstrates that a engineered vascular implant can promote angiogenesis, restore blood flow to the injured spinal cord, and promote the formation of the blood spinal cord barrier. This approach provides the foundation for studying the role of angiogenesis on regeneration and repair following SCI.

Supplementary Material

Refer to Web version on PubMed Central for supplementary material.

Acknowledgments

This work was funded through the generous support of Richard and Gail Siegal, the Discovery Eye Foundation, and the Lincy Foundation. MFR, JB, and RR acknowledge a NIH Neuroengineering Training Grant, NIH T90-DK070068. MFR would like to sincerely thank the NINDS Ohio State's Spinal Cord Injury Training Course for teaching her the spinal cord surgeries and behavioral techniques. We'd like to thank Rosh and Roshan Sethi for help with animal care. Many thanks to Dr. John Kiernan for helpful advice in eriochrome cyanine staining. We are also grateful for Dr. Jeffrey Kocsis for his patient consultations and suggestions.

Abbreviations

SCI	spinal cord injury
ECs	endothelial cells
NPCs	neural progenitor cells
BSB	blood spinal cord barrier
CNS	central nervous system

BDNF	brain derived neurotrophic factor
VEGF	vascular endothelial growth factor
EBA	endothelial barrier antigen
NO	nitric oxide
PEG	poly(ethylene glycol)
PLL	poly-L-lysine
RECA	rat endothelial cell antigen
PECAM	platelet endothelial cell adhesion molecule

REFERENCES

Bearden SE, Segal SS. Neurovascular alignment in adult mouse skeletal muscles. Microcirculation. 2005; 12:161–167. [PubMed: 15824038]

Benjamin LE. The controls of microvascular survival. Cancer and Metastasis Reviews. 2000; 19:75–81. [PubMed: 11191067]

Benowitz LI, Apostolides PJ, Perrone-Bizzozero N, Finklestein SP, Zwiers H. Anatomical Distribution of the Growth-Associated Protein GAP-43/B-50 in the Adult Rat Brain. Journal of Neuroscience. 1988; 8:339–352. [PubMed: 3339416]

Benton RL, Whittemore SR. VEGF(165) therapy exacerbates secondary damage following spinal cord injury. Neurochemical Research. 2003; 28:1693–1703. [PubMed: 14584823]

Blight AR. Morphometric Analysis of Blood-Vessels in Chronic Experimental Spinal-Cord Injury - Hypervascularity and Recovery of Function. Journal of the Neurological Sciences. 1991; 106:158–174. [PubMed: 1802964]

Cao QL, Zhang YP, Howard RM, Walters WM, Tsoulfas P, Whittemore SR. Pluripotent stem cells engrafted into the normal or lesioned adult rat spinal cord are restricted to a glial lineage. Experimental Neurology. 2001; 167:48–58. [PubMed: 11161592]

Caplan AI, Dennis JE. Mesenchymal stem cells as trophic mediators. J. Cell. Biochem. 2006; 98:1076–1084. [PubMed: 16619257]

Casella GTB, Marcillo A, Bunge MB, Wood PM. New vascular tissue rapidly replaces neural parenchyma and vessels destroyed by a contusion injury to the rat spinal cord. Experimental Neurology. 2002; 173:63–76. [PubMed: 11771939]

Engelhardt M, Wachs FP, Couillard-Despres S, Aigner L. The neurogenic competence of progenitors from the postnatal rat retina in vitro. Experimental Eye Research. 2004; 78:1025–1036. [PubMed: 15051483]

Facchiano F, Fernandez E, Mancarella S, Maira G, Miscusi M, D'Arcangelo D, Cimino-Reale G, Falchetti ML, Capogrossi MC, Pallini R. Promotion of regeneration of corticospinal tract axons in rats with recombinant vascular endothelial growth factor alone and combined with adenovirus coding for this factor. Journal of Neurosurgery. 2002; 97:161–168. [PubMed: 12134907]

Ford MC, Bertram JP, Hynes SR, Michaud M, Li Q, Young M, Segal SS, Madri JA, Lavik EB. A macroporous hydrogel for the coculture of neural progenitor and endothelial cells to form functional vascular networks in vivo. Proceedings of the National Academy of Sciences of the United States of America. 2006; 103:2512–2517. [PubMed: 16473951]

Gates MA, Thomas LB, Howard EM, Laywell ED, Sajin B, Faissner A, Gotz B, Silver J, Steindler DA. Cell and Molecular Analysis of the Developing and Adult-Mouse Subventricular Zone of the Cerebral Hemispheres. Journal of Comparative Neurology. 1995; 361:249–266. [PubMed: 8543661]

Ghabriel MN, Zhu CN, Leigh C. Electron microscope study of blood-brain barrier opening induced by immunological targeting of the endothelial barrier antigen. Brain Research. 2002; 934:140–151. [PubMed: 11955477]

Glaser J, Gonzalez R, Sadr E, Keirstead HS. Neutralization of the chemokine CXCL10 reduces apoptosis and increases axon sprouting after spinal cord injury. Journal of Neuroscience Research. 2006; 84:724–734. [PubMed: 16862543]

Gosain A, Matthies AM, Dovi JV, Barbul A, Gamelli RL, DiPietro LA. Exogenous pro-angiogenic stimuli cannot prevent physiologic vessel regression. J. Surg. Res. 2006; 135:218–225. [PubMed: 16904692]

Hermanson, GT. Bioconjugate Techniques. Academic Press; San Diego: 1996.

Hou SP, Xu QY, Tian WM, Cui FZ, Cai Q, Ma J, Lee IS. The repair of brain lesion by implantation of hyaluronic acid hydrogels modified with laminin. Journal of Neuroscience Methods. 2005; 148:60–70. [PubMed: 15978668]

Hynes S, McGregor L, Rauch M, Lavik E. Photopolymerized poly(ethylene glycol)/poly(L-lysine) hydrogels for the delivery of neural progenitor cells. J. Biomater. Sci. Polymer Edn. 2007; 18:1017–1030.

Hynes SR, Rauch MF, Bertram J, Lavik EB. A library of tunable poly(ethylene glycol)/poly-L-lysine hydrogels to investigate the materials cues that influence neural stem cell differentiation. Journal of Biomedical Materials Research Part A. accepted.

Iannotti C, Zhang YP, Shields CB, Han YC, Burke DA, Xu XM. A neuroprotective role of glial cell line-derived neurotrophic factor following moderate spinal cord contusion injury. Experimental Neurology. 2004; 189:317–332. [PubMed: 15380482]

Imperato-Kalmar EL, McKinney RA, Schnell L, Rubin BP, Schwab ME. Local changes in vascular architecture following partial spinal cord lesion in the rat. Experimental Neurology. 1997; 145:322–328. [PubMed: 9217069]

Kaneko S, Iwanami A, Nakamura M, Kishino A, Kikuchi K, Shibata S, Okano HJ, Ikegami T, Moriya A, Konishi O, Nakayama C, Kumagai K, Kimura T, Sato Y, Goshima Y, Taniguchi M, Ito M, He ZG, Toyama Y, Okano H. A selective Sema3A inhibitor enhances regenerative responses and functional recovery of the injured spinal cord. Nature Medicine. 2006; 12:1380–1389.

Kermani P, Hempstead B. Brain-derived neurotrophic factor: A newly described mediator of angiogenesis. Trends in Cardiovascular Medicine. 2007; 17:140–143. [PubMed: 17482097]

Kiernan JA. Chromoxane cyanine R. II. Staining of animal tissues by the dye and its iron complexes. J. of Microscopy. 1984; 134:25–39.

Langer R, Vacanti JP. Tissue Engineering. Science. 1993; 260:920–926. [PubMed: 8493529]

Lavik E, Langer R. Tissue engineering: current state and perspectives. Applied Microbiology and Biotechnology. 2004; 65:1–8. [PubMed: 15221227]

Lee JC, Kim DC, Gee MS, Saunders HM, Sehgal CM, Feldman MD, Ross SR, Lee WMF. Interleukin-12 inhibits angiogenesis and growth of transplanted but not in situ mouse mammary tumor virus-induced mammary carcinomas. Cancer Research. 2002; 62:747–755. [PubMed: 11830529]

Li Q, Ford MC, Lavik EB, Madri JA. Modeling the neurovascular niche: VEGF and BDNF mediated cross-talk between neural stem cells and endothelial cells: An in vitro study. Journal of Neuroscience Research. 2006; 84:1656–1668. [PubMed: 17061253]

Loy DN, Crawford CH, Darnall JB, Burke DA, Onifer SM, Whittemore SR. Temporal progression of angiogenesis and basal lamina deposition after contusive spinal cord injury in the adult rat. Journal of Comparative Neurology. 2002; 445:308–324. [PubMed: 11920709]

Lu B, Kwan T, Kurimoto Y, Shatos M, Lund RD, Young MJ. Transplantation of EGF-responsive neurospheres from GFP transgenic mice into the eyes of rd mice. Brain Research. 2002; 943:292–300. [PubMed: 12101053]

Lu P, Jones LL, Snyder EY, Tuszynski MH. Neural stem cells constitutively secrete neurotrophic factors and promote extensive host axonal growth after spinal cord injury. Experimental Neurology. 2003; 181:115–129. [PubMed: 12781986]

Madri J, Williams S. Capillary Endothelial Cell Cultures: Phenotypic Modulation by Matrix Components. The Journal of Cell Biology. 1983; 97:153–165. [PubMed: 6190818]

Mahooti S, Graesser D, Patil S, Newman P, Duncan G, Mak T, Madri JA. PECAM-1 (CD31) expression modulates bleeding time in vivo. American Journal of Pathology. 2000; 157:75–81. [PubMed: 10880378]

Mautes A, Weinzierl M, Donovan F, Noble L. Vascular Events After Spinal Cord Injury: Contribution to Secondary Pathogenesis. Physical Therapy. 2000; 80:673–687. [PubMed: 10869130]

Mondrinos MJ, Koutzaki SH, Poblete HM, Crisanti MC, Lelkes PI, Finck CM. In vivo pulmonary tissue engineering: Contribution of donor-derived endothelial cells to construct vascularization. Tissue Engineering Part A. 2008; 14:361–368. [PubMed: 18333788]

Morshead CM, Reynolds BA, Craig CG, McBurney MW, Staines WA, Morassutti D, Weiss S, Vanderkooy D. Neural Stem-Cells in the Adult Mammalian Forebrain - a Relatively Quiescent Subpopulation of Subependymal Cells. Neuron. 1994; 13:1071–1082. [PubMed: 7946346]

Nor JE, Peters MC, Christensen JB, Sutorik MM, Linn S, Khan MK, Addison CL, Mooney DJ, Polverini PJ. Engineering and characterization of functional human microvessels in immunodeficient mice. Lab Invest. 2001; 81:453–463. [PubMed: 11304564]

Ogunshola OO, Stewart WB, Mihalcik V, Solli T, Madri JA, Ment LR. Neuronal VEGF expression correlates with angiogenesis in postnatal developing rat brain. Dev. Brain Res. 2000; 119:139–153. [PubMed: 10648880]

Ohab JJ, Fleming S, Blesch A, Carmichael ST. A neurovascular niche for neurogenesis after stroke. Journal of Neuroscience. 2006; 26:13007–13016. [PubMed: 17167090]

Pallini R, Vitiani LR, Bez A, Casalbore P, Facchiano F, Gerevini VD, Falchetti ML, Fernandez E, Maira G, Peschle C, Parati E. Homologous transplantation of neural stem cells to the injured spinal cord of mice. Neurosurgery. 2005; 57:1014–1024. [PubMed: 16284571]

Patist CM, Mulder MB, Gautier SE, Maquet V, Jerome R, Oudega M. Freeze-dried poly(D,L-lactic acid) macroporous guidance scaffolds impregnated with brain-derived neurotrophic factor in the transected adult rat thoracic spinal cord. Biomaterials. 2004; 25:1569–1582. [PubMed: 14697859]

Perdiki M, Farooque M, Holtz A, Li GL, Olsson Y. Expression of endothelial barrier antigen immunoreactivity in blood vessels following compression trauma to rat spinal cord - Temporal evolution and relation to the degree of the impact. Acta Neuropathologica. 1998; 96:8–12. [PubMed: 9678508]

Peters MC, Polverini PJ, Mooney DJ. Engineering vascular networks in porous polymer matrices. Journal of Biomedical Materials Research. 2002; 60:668–678. [PubMed: 11948526]

Pinter E, Mahooti S, Wang Y, Imhof BA, Madri JA. Hyperglycemia-induced vasculopathy in the murine vitelline vasculature - Correlation with PECAM-1/CD31 tyrosine phosphorylation state. American Journal of Pathology. 1999; 154:1367–1379. [PubMed: 10329590]

Raab S, Plate KH. Different networks, common growth factors: shared growth factors and receptors of the vascular and the nervous system. Acta Neuropathologica. 2007; 113:607–626. [PubMed: 17492293]

Rauch MF, Michaud M, Xu H, Madri JA, Lavik EB. Coculture of primary neural progenitor and endothelial cells in a synthetic, degradable macroporous gel promotes stable vascular networks in vivo. Journal of Biomaterials Science-Polymer Edition. accepted.

Richardson TP, Peters MC, Ennett AB, Mooney DJ. Polymeric system for dual growth factor delivery. Nature Biotechnology. 2001; 19:1029–1034.

Sasaki M, Hains BC, Lankford KL, Waxman SG, Kocsis JD. Protection of corticospinal tract neurons after dorsal spinal cord transection and engraftment of olfactory ensheathing cells. Glia. 2006; 53:352–359. [PubMed: 16288464]

Simard M, Arcuino G, Takano T, Liu QS, Nedergaard M. Signaling at the gliovascular interface. Journal of Neuroscience. 2003; 23:9254–9262. [PubMed: 14534260]

Skold M, Cullheim S, Hammarberg H, Piehl F, Suneson A, Lake S, Sjogren A, Walum E, Risling M. Induction of VEGF and VEGF receptors in the spinal cord after mechanical spinal injury and prostaglandin administration. European Journal of Neuroscience. 2000; 12:3675–3686. [PubMed: 11029637]

Sternberger NH, Sternberger LA. Blood-Brain-Barrier Protein Recognized by Monoclonal-Antibody. Proceedings of the National Academy of Sciences of the United States of America. 1987; 84:8169–8173. [PubMed: 3500474]

Su JJ, Osoegawa M, Matsuoka T, Minohara M, Tanaka M, Ishizu T, Mihara F, Taniwaki T, Kira J. Upregulation of vascular growth factors in multiple sclerosis: Correlation with MRI findings. Journal of the Neurological Sciences. 2006; 243:21–30. [PubMed: 16376944]

Teng YD, Lavik EB, Qu XL, Park KI, Ourednik J, Zurakowski D, Langer R, Snyder EY. Functional recovery following traumatic spinal cord injury mediated by a unique polymer scaffold seeded with neural stem cells. Proceedings of the National Academy of Sciences of the United States of America. 2002; 99:3024–3029. [PubMed: 11867737]

Terpstra BT, Collier TJ, Marchionini DM, Levine ND, Paumier KL, Sortwell CE. Increased cell suspension concentration augments the survival rate of grafted tyrosine hydroxylase immunoreactive neurons. Journal of Neuroscience Methods. 2007; 166:13–19. [PubMed: 17706789]

Tomita M, Lavik E, Klassen H, Zahir T, Langer R, Young MJ. Biodegradable polymer composite grafts promote the survival and differentiation of retinal progenitor cells. Stem Cells. 2005; 23:1579–1588. [PubMed: 16293582]

Tremblay PL, Hudon V, Berthod F, Germain L, Auger FA. Inosculation of tissue-engineered capillaries with the host's vasculature in a reconstructed skin transplanted on mice. American Journal of Transplantation. 2005; 5:1002–1010. [PubMed: 15816880]

Whetstone WD, Hsu JYC, Eisenberg M, Werb Z, Noble-Haeusslein LJ. Blood-spinal cord barrier after spinal cord injury: Relation to revascularization and wound healing. Journal of Neuroscience Research. 2003; 74:227–239. [PubMed: 14515352]

Widenfalk J, Lipson A, Jubran M, Hofstetter C, Ebendal T, Cao Y, Olson L. Vascular endothelial growth factor improves functional outcome and decreases secondary degeneration in experimental spinal cord contusion injury. Neuroscience. 2003; 120:951–960. [PubMed: 12927201]

Widenfalk J, Lundstromer K, Jubran M, Brene S, Olson L. Neurotrophic factors and receptors in the immature and adult spinal cord after mechanical injury or kainic acid. Journal of Neuroscience. 2001; 21:3457–3475. [PubMed: 11331375]

Willis CL, Leach L, Clarke GJ, Nolan CC, Ray DE. Reversible disruption of tight junction complexes in the rat blood brain barrier, following transitory focal astrocyte loss. Glia. 2004; 48:1–13. [PubMed: 15326610]

Yoshihara T, Ohta M, Itokazu Y, Matsumoto N, Dezawa M, Suzuki Y, Taguchi A, Watanabe Y, Adachi Y, Ikehara S, Sugimoto H, Ide C. Neuroprotective effect of bone marrow-derived mononuclear cells promoting functional recovery from spinal cord injury. Journal of Neurotrauma. 2007; 24:1026–1036. [PubMed: 17600518]

Zacchigna S, Lambrechts D, Carmeliet P. Neurovascular signalling defects in neurodegeneration. Nature Reviews Neuroscience. 2008; 9:169–181.

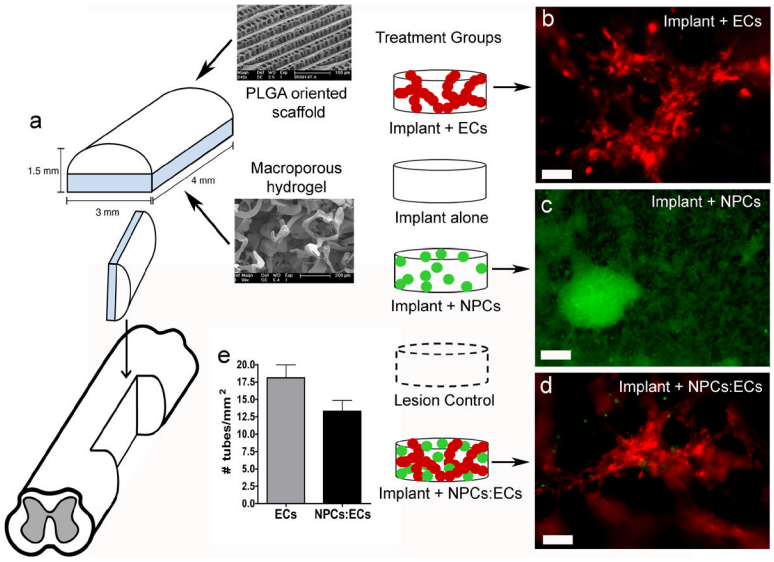

Figure 1. Implant design

(a) Two component implant includes an outer PLGA oriented scaffold and an inner PEG/PLL macroporous hydrogel. (b) Live image of DiI-labeled rat ECs (red) cultured on a macroporous gel for one day. (c) Live image of GFP-positive rat NPCs (green) cultured on a macroporous gel for seven days. (d) Live image of DiI-labeled rat ECs (red) and GFP-positive rat NPCs (green) cultured on a macroporous gel for one day. Scale bar in (b–d) is 100 μm. (e) The number of EC tubes in the implant plus ECs and implant plus NPCs:ECs groups implanted into the hemisected spinal cord.

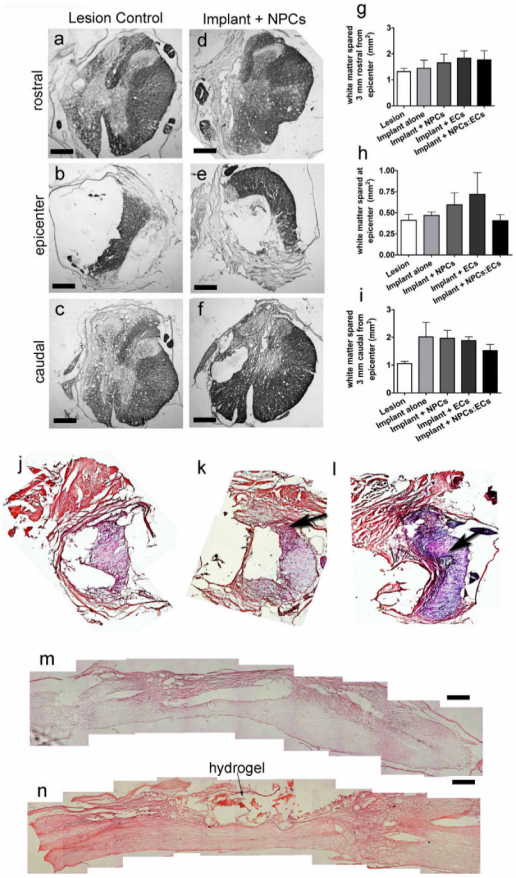

Figure 2. Eriochrome cyanine to determine white matter spared and H&E results

(a–f) Representative ECy stained cross sections from a lesion control and an implant plus NPCs cord rostral, at, and caudal to the injury epicenter. Scale bar = 400 μm. Graphs of the mean area of white matter spared 3 mm rostral from the epicenter (g), at the lesion epicenter (h), and 3 mm caudal from the epicenter (i) show that amount of white matter spared is similar for all groups. Error bars = ± SEM. (j) H&E of the epicenter of a lesion control cord. (k) H&E of the injury epicenter of an implant alone cord with an arrow noting the residual grey matter. (l) H&E of the injury epicenter of an implant plus NPCs:ECs cord. A small amount of grey matter can be seen lining the lesion (arrow). The lesioned side is on the left in all of the cross sections. (m) H&E of a longitudinal section of a lesion control cord. The left, hemisected side is at the top of the image. Scale bar = 1 mm. (n) H and E of a longitudinal section of an implant plus NPCs cord. The hydrogel can be seen in the hemisected region in this image. This section is a sister section of the longitudinal image in Fig. 7g. Scale bar = 1 mm.

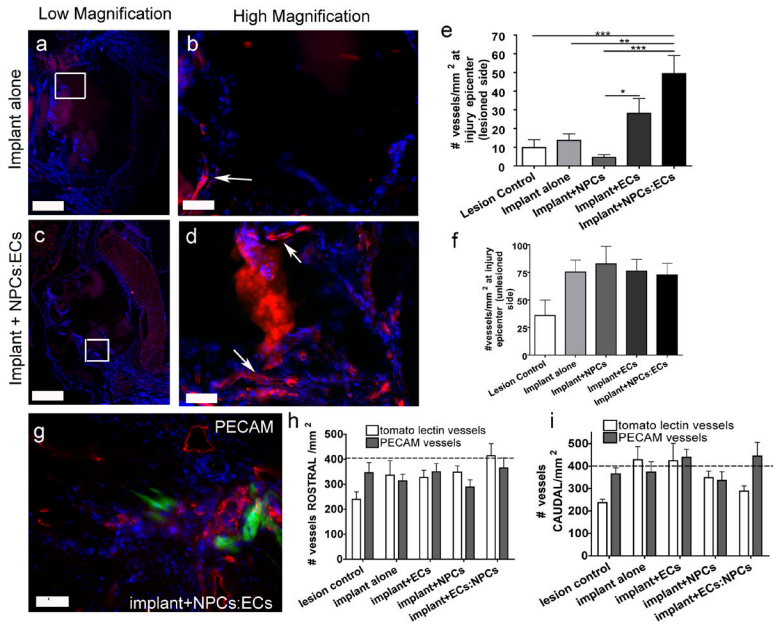

Figure 3. Functional vessels at the lesion epicenter

All images are spinal cord cross sections in which vessels perfused with biotinylated lectin are labeled with streptavidin-Texas Red and nuclei are labeled blue with DAPI. (a) Low magnification image from the implant alone group. The white box in (a) denotes the region viewed in (b). (b) High magnification image of white box in (a) showing labeled vessels (white arrows). (c) Low magnification image from an implant plus NPCs:ECs group. **The white box denotes the region viewed in (d).** (d) High magnification of white box in (c) showing vessels which are further marked with white arrows. Scale bars in (a) and (c) are 400 μm. Scale bars in (b) and (d) are 50 μm. (e) Number of vessels/mm^2 on the lesioned at the injury epicenter. (f) The number of vessels/mm^2 on the unlesioned side at the injury epicenter. (g) PECAM-1 staining of am implant plus NPCs:ECs section on the lesioned side of the injury epicenter. The green cells are NPCs. Scale bar = 50 μm (h) Quantification of tomato lectin and PECAM vessels 3.6 mm rostral to the injury epicenter and (i) 3.6 mm caudal to the injury epicenter. The dotted line denotes the approximate number of vessels found in the grey matter of a normal spinal cord. Error bars = ± SEM. * = $p<0.05$, ** = $p<0.01$, *** = $p<0.001$.

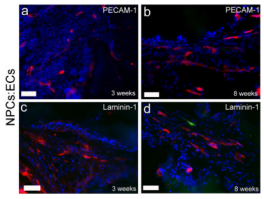

Figure 4. PECAM-1 and laminin-1 positive vessels at early and late time points

Representative images of cross-sections from an implant plus NPCs:ECs group immunostained for PECAM-1 and laminin-1. Similar morphologies were seen for all groups. All images are from the lesioned side at the injury epicenter. (a) PECAM-1 (red) at three weeks and (b) eight weeks. Laminin-1 (red) staining at (c) three weeks and (d) eight weeks. The green cell in (d) is an NPC. Sections are counterstained with DAPI (blue). Scale bars are 50 μm.

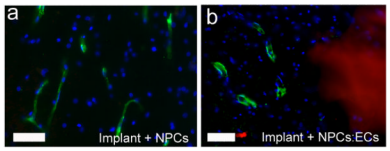

c Number of cords with EBA+ vessels/Total cords in cross-sectional analysis

Group	Unlesioned side	Lesioned side
Lesion control	3/5	0/5
Implant alone	3/5	0/5
Implant + NPCs	5/5	0/5
Implant + ECs	2/5	0/5
Implant + NPCs:ECs	5/5	4/5

d Average number of EBA+ vessels/mm^2

Group	Unlesioned side	Lesioned side
Lesion control	24 ± 11	0
Implant alone	39 ± 18	0
Implant + NPCs	46 ± 16	0
Implant + ECs	15 ± 6	0
Implant + NPCs:ECs	29 ± 6	18 ± 6

Figure 5. EBA-positive vessels

(a) Cross-section image on the unlesioned side of EBA-positive vessels from a representative implant plus NPCs cord. (b) Cross-section image on the lesioned side of EBA-positive vessels from an implant plus NPCs:ECs cord. The nuclei are labeled with DAPI (blue), EBA-positive vessels are green, and the hydrogel in (b) is autofluorescing in the red channel. Scale bars are 50 μm. (c) Table of the number of cords per total cords cross sectioned with EBA-positive vessels at the injury epicenter. (d) Table of the average number of EBA-positive vessels ± S.E.M. at the lesion epicenter on both the lesioned and unlesioned side of the spinal cord. Only the implant plus NPCs:ECs has EBA-positive vessels on the lesioned side at the injury epicenter.

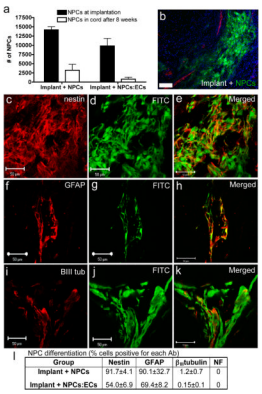

Figure 6. NPC survival and differentiation

(a) Graph of the total number of NPCs at implantation compared to the total number of NPCs found in the spinal cord at eight weeks. (b) Image demonstrating GFP-positive NPCs in the cord as well as their close association with streptavidin-Texas Red labeled blood vessels (red). (c–k) Confocal images of longitudinal sections in which NPCs were found in the injury epicenter in the implant or in tissue adjacent to the implant. (c–e) GFP-positive NPCs (d) stained positively with nestin (c). (e) Merged image of (c) and (d). (f–h) GFP-positive NPCs (g) expressed GFAP (f). (h) Merged image of (f) and (g). (i–k) Representative image of GFP-positive NPCs (j) expressing ®$_{III}$ tubulin (i). (k) Merged image of (i) and (j). (l) Table of the % of cells (± S.E.M.) in the spinal cord positive for each antibody.

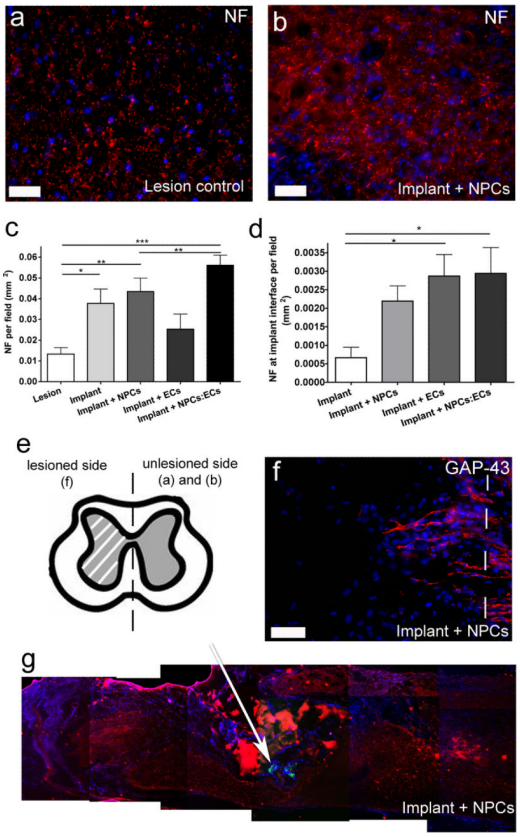

Figure 7. Neurofilament immunostaining and GAP-43

NF-positive neurons are red and DAPI-labeled cells nuclei are blue. A cross section at the injury epicenter on the unlesioned side from the lesion control (a) and implant plus NPCs groups (b). (c) Graph of the mean area of NF-positive cells on the unlesioned side at the lesion epicenter per 20X field. Error bars = ± SEM. * = $p<0.05$, ** = $p<0.01$, and *** = $p<0.001$. (d) Graph of the area of NF-positive cells at the implant/host interface. * = $p<0.05$ The implant plus ECs and implant plus ECs:NPCs show significantly more ingrowth than the implant alone group. (e) Schematic of a cross-section showing where the images are from in the tissue. (f) A longitudinal section from an implant plus NPCs cord showing GAP-43 fibers extending from the unlesioned side (right side of dotted line) into the lesion (left side of dotted line). (g) Longitudinal section stained with NF (red) and DAPI (blue). This is the sister section to the longitudinal image in Fig. 2n. GFP-positive NPCs are seen in the gel (white arrow). The red patches in (g) are remnants of the hydrogel that are autofluorescing. Scale bars in (a), (b) and (f) are 50 μm.